



Title	Development and validation of a prediction model based on the organ-based metabolic tumor volume on FDG-PET in patients with differentiated thyroid carcinoma
Author(s)	Uchiyama, Yuko; Hirata, Kenji; Watanabe, Shiro; Okamoto, Shozo; Shiga, Tohru; Okada, Kazufumi; Ito, Yoichi M.; Kudo, Kohsuke
Citation	Annals of nuclear medicine, 35(11), 1223-1231 https://doi.org/10.1007/s12149-021-01664-x
Issue Date	2021-11-01
Doc URL	http://hdl.handle.net/2115/87316
Rights	This is a post-peer-review, pre-copyedit version of an article published in Annals of nuclear medicine. The final authenticated version is available online at: http://dx.doi.org/10.1007/s12149-021-01664-x .
Type	article (author version)
File Information	Ann Nucl Med 35(11) 1223-1231.pdf



[Instructions for use](#)

1 Title

2 **Development and validation of a prediction model based on the organ-based metabolic**
3 **tumor volume on FDG-PET in patients with differentiated thyroid carcinoma**

4

5 Authors

6 Yuko Uchiyama, MD,^{1,2} Kenji Hirata, MD, PhD,^{1,2,*} Shiro Watanabe, MD, PhD,^{1,2} Shozo

7 Okamoto, MD, PhD,³ Tohru Shiga, MD, PhD,⁴ Kazufumi Okada, MPH,⁵ Yoichi M. Ito, PhD,⁵

8 Kohsuke Kudo, MD, PhD^{1,6,7}

9

10 ¹Department of Diagnostic Imaging, Hokkaido University Graduate School of Medicine,
11 Sapporo, Japan

12 ²Department of Nuclear Medicine, Hokkaido University Hospital, Sapporo, Japan

13 ³Department of Radiology, Obihiro-Kosei General Hospital, Obihiro, Japan

14 ⁴Advanced Clinical Research Center, Fukushima Global Medical Science Center, Fukushima,
15 Japan

16 ⁵Biostatistics Division, Clinical Research and Medical Innovation Center, Hokkaido University
17 Hospital, Sapporo, Japan

18 ⁶Department of Diagnostic Imaging and Interventional Radiology, Hokkaido University
19 Hospital, Sapporo, Japan

20 ⁷Global Center for Biomedical Science and Engineering, Faculty of Medicine, Hokkaido
21 University, Sapporo, Japan

22

23

24 **First author:** Yuko Uchiyama, MD, PhD candidate, Department of Diagnostic Imaging,
25 Graduate School of Medicine, Hokkaido University, Kita 15, Nishi 7, Kita-Ku, Sapporo,
26 Hokkaido 060-8638, Japan. Tel.: +81-11-706-7779, Fax: +81-11-706-7408
27 Email: y_uchiyama@med.hokudai.ac.jp

28
29 ***Corresponding author:** Dr. Kenji Hirata, Department of Diagnostic Imaging, Graduate School
30 of Medicine, Hokkaido University, Kita 15, Nishi 7, Kita-Ku, Sapporo, Hokkaido 060-8638,
31 Japan.
32 Tel.: +81-11-706-7779, Fax: +81-11-706-7408
33 Email: khirata@med.hokudai.ac.jp

34
35 **Source of Funding:**

36 This work was supported by a grant from the JSPS KAKENHI, no. JP20K08015.

37
38 **Running Title:** Organ-based MTV in thyroid cancer

39
40 **Total word count:** 4081

41
42 Total number of figures: 5

43 Total number of tables: 3

44

45

46 **ABSTRACT**

47 **Background:** Although patients with differentiated thyroid cancer (DTC) generally have a good
48 prognosis, patients with a large metabolic tumor volume (MTV) on FDG-PET may experience
49 poor clinical courses. We measured organ-based MTVs and tested its prognostic performance in
50 comparison to conventional MTV (cMTV).

51 **Methods:** We retrospectively analyzed the cases of 280 patients who received their first I-131
52 therapy in 2003–2014 at our hospital and showed an FDG-avid metastatic lesion. We randomly
53 divided the patients into training (n=190) and validation (n=90) datasets. We classified the MTVs
54 as $MTV_{\text{neck-node}}$, $MTV_{\text{distant-node}}$, MTV_{lung} , MTV_{bone} , and $MTV_{\text{other-organs}}$ and tested with/without
55 dichotomization vis-à-vis overall survival (OS). Based on the estimated weighting coefficients of
56 the organ-based MTVs, we propose a new index: the adjusted whole-body MTV (aMTV). Using
57 the validation dataset, we compared the aMTV with cMTV for predicting OS.

58 **Results:** In a univariate analysis, $MTV_{\text{distant-node}}$ and $MTV_{\text{other-organs}}$ were more strongly correlated
59 with the OS than the dichotomized forms, whereas the dichotomized forms of $MTV_{\text{neck-node}}$,
60 MTV_{lung} , and MTV_{bone} were more strongly correlated with OS than the continuous variables. The
61 aMTV was thus expressed as $0.69 \times \text{dic}(MTV_{\text{neck-node}}) + 0.02 \times MTV_{\text{distant-node}}$
62 $+ 1.05 \times \text{dic}(MTV_{\text{lung}}) + 1.58 \times \text{dic}(MTV_{\text{bone}}) + 0.01 \times MTV_{\text{other-organs}}$, where $\text{dic}(x)$ represents 0 or
63 1 based on the optimized cut-off. In the model evaluation using the validation group, aMTV was
64 a significant predictor of OS with a higher c-index (0.7676) than cMTV (0.7218).

65 **Conclusion:** In DTC patients with FDG-avid metastasis before I-131 therapy, all organ-based
66 MTVs were significant predictors of prognosis. As the aMTV outperformed the cMTV for
67 predicting prognoses, we recommend measuring the MTV on an organ basis.

68

69 **Key words**

70 differentiated thyroid carcinoma, metabolic tumor volume, organ-based measurement, FDG-PET

71

72 **Introduction**

73 Patients with differentiated thyroid cancer (DTC) have a relatively good prognosis with
74 slow progress in most cases, but there is a group of DTC patients who experience a poor clinical
75 course. The known clinical factors associated with poor prognosis in DTC include a large
76 primary lesion, advanced patient age at the first diagnosis, male sex, and the presence of
77 metastasis [1, 2]. F-18 fluorodeoxyglucose (FDG) positron emission tomography (PET) is a
78 useful clinical tool to predict the prognosis of DTC patients, as in other malignancies. It has been
79 clarified those patients with FDG-avid metastasis had worse prognoses than those without FDG-
80 avid metastasis [3, 4].

81 Metabolic tumor volume (MTV) and total lesion glycolysis (TLG) derived from FDG-
82 PET/CT have been reported to be good prognostic factors for various malignant tumors [5–7].
83 There have also been reports that a higher MTV and TLG in FDG-PET are factors associated
84 with poor prognosis in DTC [8, 9]. However, it has been indicated that in cases of DTC, the neck
85 lymph nodes have little effect on the patients' overall survival (OS) [10], and that the prognosis is
86 poor when the patient has distant metastasis in organs that are not commonly targets of
87 metastasis, such as the liver and brain [11, 12]. These lines of evidence suggest that, even if their
88 MTV values are equal, metastatic lesions that have developed at different organs may have
89 different clinical impacts. Nevertheless, most of the investigations of the MTV and TLG have
90 considered all metastatic lesions equally, i.e., the whole-body MTV calculated as the sum of the
91 individual lesions' MTVs throughout the body is most commonly used. We hypothesized that
92 both MTV measurements obtained in an organ-by-organ manner and the organ-adjusted whole-
93 body MTV, defined as the weighted sum of the organ-based MTVs, may have better prognostic
94 performance.

95 In this retrospective study, we aimed to develop an organ-based MTV-based model and to
96 determine whether it is more useful for predicting the prognosis of patients with DTC compared
97 to the conventional MTV.

98

99 **Subjects and Methods**

100 *Subjects*

101 Based on the Transparent Reporting of Multivariate Prediction Model for Individual Prognosis or
102 Diagnosis (TRIPOD) statement, the present study is categorized as type 2a [13]. This
103 retrospective analysis was approved by our hospital's institutional review board (approval no.
104 020-0315). The requirement of written informed consent from each patient was waived because
105 of the study's retrospective nature. We reviewed our hospital's information system to extract the
106 cases of patients who underwent FDG-PET or PET/CT at our hospital before undergoing I-131
107 radioactive iodine therapy (RAI) for DTC between January 2003 and December 2014.

108 Based on the results of a computer-based search of the hospital's medical records, a total
109 of 1,218 RAI treatments for 800 patients were performed for DTC during that period. Among
110 them, 767 RAI treatments were identified as the first RAI after total thyroidectomy, and 33 RAI
111 treatments were performed as the second or later RAI. Among the 767 cases of first RAI
112 treatments, 425 patients proved to have one or more residual metastatic lesions in an examination
113 before their RAI (details are provided below in the *Visual assessment of FDG-PET* section). Of
114 these 425 patients, 290 showed any FDG-avid metastatic lesion in any organs; 10 of the patients
115 were excluded as we could not access their clinical data. A final total of 280 patients (187
116 females [67%], 93 males [23%]) were enrolled (Fig. 1).

117 The mean \pm SD patient age was 60.4 ± 13.5 years (range 13–84 years; median 64,

118 interquartile range [IQR]: 54–69 years). The data on patient survival during the follow-up period
119 after FDG-PET were collected through routine clinical visits and telephone interviews. The
120 follow-up period ranged from 1.13 to 154.8 months (median 54.5, IQR: 26.5–94.1 months). No
121 patients were treated by a tyrosine kinase inhibitor (TKI) within the observation period.

122

123 *Image acquisition*

124 After 6-hr fasting and blood glucose measurement, the patient was injected with FDG (4.5
125 MBq/kg), followed by whole-body scanning 1 hr after the injection. Three different PET or PET-
126 CT scanners were used in this cohort: (1) an ECAT EXACT HR+ PET scanner (Siemens,
127 Munich, Germany) (n=14 patients), (2) an ECAT EXACT 47 PET scanners (Siemens) (n=128),
128 and (3) a Biograph 64 PET/CT scanner (Siemens) (n=138).

129 For the ECAT EXACT HR+ and ECAT EXACT 47 PET scanners, 2-min emission
130 scanning and 2-min transmission scanning with a $^{68}\text{Ge}/^{68}\text{Ga}$ source per bed position were
131 performed, followed by image reconstruction using ordered subset expectation maximization
132 (OSEM, 1 iteration, 30 subsets). For the Biograph 64 PET/CT scanner, low-dose CT images
133 were acquired for attenuation correction, followed by 3-min emission scanning for each bed
134 position. PET images were reconstructed using the TrueX algorithm, which is a point spread
135 function implemented in OSEM (two iterations, 21 subsets). After reconstruction, the matrix
136 sizes were 128×128 for both ECAT scanners and 168×168 for the Biograph64, and the voxel
137 sizes were $3.4 \times 3.4 \times 3.4$ mm for both ECAT scanners and $4.1 \times 4.1 \times 2.0$ mm for the Biograph64.

138

139 *Visual assessment of FDG-PET*

140 The accumulation of FDG was visually evaluated and discussed by two board-certificated

141 nuclear medicine physicians (Y.U. and K.H., 18 years and 15 years of experience, respectively)
142 to determine each patient's inclusion in this study. To evaluate the presence/absence of metastasis
143 and metastatic organs, we collected each patient's serum thyroglobulin (sTg) level and findings
144 from imaging examinations such as computed tomography (CT), magnetic resonance imaging
145 (MRI), and ultrasonography (US) taken essentially within 1 month before RAI treatment, and the
146 I-131 scintigraphy after the patient's initial therapy. The lesion was judged to be an FDG-avid
147 metastatic lesion if it exhibited FDG uptake greater than that of the surrounding tissues.

148

149 *Semi-quantitative analysis*

150 For the image analysis, we used a free software package, Metavol [14]. First, any uptake masses
151 with a standardized uptake value (SUV) ≥ 3.0 were automatically extracted. Then, the nuclear
152 medicine physician with 18 years' experience categorized each uptake mass into 'tumor uptake'
153 or 'non-tumor uptake.' In cases in which the tumor and non-tumor masses were connected, the
154 non-tumor parts were carefully removed with the use of a manual region-of-interest tool. The
155 same physician then categorized each tumor uptake by the organs.

156 We defined the organ-based MTV as the tumor volume at each organ, including neck
157 node(s) ($MTV_{\text{neck-node}}$), distant node(s) ($MTV_{\text{distant-node}}$, i.e., lymph nodes beyond the neck), lung
158 (MTV_{lung}), bone (MTV_{bone}), and other organs ($MTV_{\text{other-organs}}$). The 'other organs' included the
159 liver (n=3), pleura (n=5), muscle (n=1), and kidney (n=1). A representative case is illustrated in
160 Fig. 2.

161

162 *Statistical analyses*

163 The statistical analyses were performed using JMP Pro 14 and SAS 9.4 (SAS Institute Inc., Cary,

164 NC, USA) in the following three steps after we randomly divided all 280 patients into two
165 groups (training, n=190; validation, n=90). The randomization was performed using Microsoft
166 Excel. In the analyses described next, the training dataset was used in (i), (ii), and (iii), and the
167 validation dataset was used in (iii).

168

169 i) Univariate analysis

170 We first performed a univariate analysis to test the prognostic value of each organ-based MTV.
171 The Cox proportional hazard model was used to input the organ-based MTV as the single
172 explanatory variable and to output the patients' overall survival (OS) as a response variable. We
173 exhaustively searched for the best cut-off value to dichotomize each organ-based MTV. The cut-
174 off value was adjusted by 0.1 mL until the dichotomized form of the organ-based MTV became
175 the most prognostic (i.e., showed the highest c-index). The continuous form or the dichotomized
176 form of each organ-based MTV, whichever was observed to be more predictive, was used for the
177 subsequent analyses.

178

179 ii) Multivariate analysis (multivariate model construction)

180 We then constructed a Cox proportional hazard model to input the five organ-based MTVs to
181 predict OS. The estimated regression coefficients were used as the weighting coefficients for a
182 score calculation.

183

184 iii) Model validation

185 The constructed model was evaluated using the validation dataset. Using the weighting
186 coefficients that were determined as described above, we defined the weighted sum of the five

187 organ-based MTVs as the 'adjusted whole-body MTV' (aMTV). For comparison, the simple sum
188 of the organ-based MTVs was defined as the 'conventional MTV' (cMTV). Both the aMTV and
189 cMTV were tested by a univariate Cox regression proportional hazard model with the OS as a
190 dependent variable.

191 The patients' OS was analyzed by the Kaplan-Meier method with the log-rank test. For the
192 univariate and multivariate analyses, p-values <0.05 were accepted as significant. The data of the
193 patient groups in the Results section are presented as the range (median, IQR).

194 We also determined the time-dependent receiver operating characteristic (ROC) curve
195 and area under the curve (AUC) of the ROC for the patients' 1-year, 3-year, and 5-year survival
196 in both the training and validation datasets to evaluate the prognostic performance of the aMTV
197 compared to the cMTV.

198

199 **Results**

200 *Patient characteristics*

201 Overall, 71 of the 280 (25.0%) patients died during the follow-up period (median 54.5 months),
202 resulting in 5- and 10-year OS rates of 81.6% and 53.6%, respectively. The characteristics of the
203 included patients are summarized in Table 1. Briefly, the training group consisted of 66 male and
204 124 female patients: the validation group was 27 male and 63 female patients. The ages of the
205 patients in the training group ranged from 13 to 84 years (median 64 yrs, IQR 56–70 yrs); those
206 for the patients in the test group were 14–80 years (median 62 yrs, IQR 51.8–69 yrs). There were
207 no significant differences between the training and test groups in age, sex, or distribution of
208 metastatic organs. The range of follow-up periods of the training group was 1.15–154.8 months
209 (median 53.9, IQR 25.2–92.6 mos.) and 2.66–153.1 months (median 56.6, IQR 30.5–95.9 mos.)

210 for the test group. Among the 71 patients who died during the follow-up period, 51 belonged to
211 the training group and 20 to the test group.

212

213 *Univariate analysis*

214 The results of univariate analysis of organ-based MTVs for OS prediction are summarized in the
215 Table 2. When each organ-based MTV was used as a continuous variable, c-indexes were 0.5454
216 ($MTV_{\text{neck-node}}$), 0.6046 ($MTV_{\text{distant-node}}$), 0.5708 (MTV_{lung}), 0.5252 (MTV_{bone}), and 0.5596
217 ($MTV_{\text{other-organ}}$). We dichotomized these MTVs by using the best cut-off values searched in 0.1-
218 mL steps. The best cut-offs were 2.9 mL for $MTV_{\text{neck-node}}$ (c-index = 0.5841), 0.3 mL for
219 $MTV_{\text{distant-node}}$ (c-index = 0.6026), 1.5 mL for MTV_{lung} (c-index = 0.5784), 15.5 mL for MTV_{bone}
220 (c-index = 0.5419), and 0.1 mL for $MTV_{\text{other-organs}}$ (c-index = 0.5593).

221

222 *Multivariate analysis (multivariate model construction)*

223 We compared the c-indexes between each organ-based MTV's continuous form and its
224 dichotomized form (i.e., without vs. with dichotomization). The form that provided the higher c-
225 index was used for the subsequent multivariate analysis. Based on the results described above,
226 $MTV_{\text{distant-node}}$ and $MTV_{\text{other-organs}}$ as continuous variables and $MTV_{\text{neck-node}}$, MTV_{lung} , and
227 MTV_{bone} as dichotomized variables were selected as the input for a multivariate analysis. The
228 estimated weighting coefficients was calculated as 0.69 for $\text{dic}(MTV_{\text{neck-node}})$, 0.02 for $MTV_{\text{distant-}}$
229 $node$, 1.05 for $\text{dic}(MTV_{\text{lung}})$, 1.58 for $\text{dic}(MTV_{\text{bone}})$, and 0.01 for $MTV_{\text{other-organs}}$ (Table 3). Note
230 that $\text{dic}(x)$ indicates 0 when $x < \theta$ and 1 when $x \geq \theta$ with θ being the cut-off determined in the
231 univariate analysis.

232 We thus defined the aMTV (adjusted whole-body MTV) as follows:

233

$$\begin{aligned} 234 \quad \text{aMTV} &= 0.69 \times \text{dic}(\text{MTV}_{\text{neck-node}}) + 0.02 \times \text{MTV}_{\text{distant-node}} \\ 235 \quad &+ 1.05 \times \text{dic}(\text{MTV}_{\text{lung}}) + 1.58 \times \text{dic}(\text{MTV}_{\text{bone}}) + 0.01 \times \text{MTV}_{\text{other-organs}} \end{aligned}$$

236

237 *Model validation*

238 Lastly, we evaluated the prognostic performance of the aMTV compared to the cMTV, using the
239 validation dataset. As a result of the univariate analysis to predict OS, the c-index of the aMTV
240 was 0.7676, which was higher than that of the cMTV (0.7218). In the results of the survival
241 analysis with Kaplan-Meier curves using the log-rank test to divide the data into two groups
242 using the median, both aMTV and cMTV were prognostic factors ($p=0.0002$ and $p=0.0006$,
243 respectively) (Fig. 3).

244 The time-dependent ROC analysis to predict 1-year, 3-year, and 5-year survival in the
245 training dataset demonstrated that the aMTV had larger AUCs than the cMTV in the training
246 dataset (Fig. 4). The respective AUC values of the aMTV and cMTV were 0.7436 vs. 0.5169 for
247 1-year survival, 0.6855 and 0.5687 for 3-year survival, and 0.6553 and 0.5679 for 5-year
248 survival. Similarly, the aMTV produced larger AUC values than the cMTV in the validation
249 dataset (Fig. 5). The respective AUC values of the aMTV and cMTV for the validation dataset
250 were 0.8566 and 0.7846 for 1-year survival, 0.7568 and 0.6528 for 3-year survival, and 0.7867
251 and 0.6314 for 5-year survival.

252

253 **Discussion**

254 We investigated the usefulness of organ-based MTVs over the conventional MTV measured on
255 FDG-PET in patients with DTC. The results can be summarized as follows. (1) The univariate

256 analysis suggested that $MTV_{\text{distant-node}}$ and $MTV_{\text{other-organs}}$ as continuous variables and $MTV_{\text{neck-}}$
257 $node$, MTV_{lung} , and MTV_{bone} as dichotomized variables were significant prognostic factors. (2)
258 With the multivariate analysis, we estimated weighting factors of each organ-based MTV. (3)
259 Using the weighting factors and the separated test dataset, we observed that the aMTV was
260 superior to the cMTV in terms of predicting the OS of the patients.

261 Volume-based parameters of FDG-PET/CT, such as MTV and TLG, have been shown to
262 be useful for prognostic factors in various malignant tumors [15–17]. This also applies to thyroid
263 cancer. However, few reports have focused on organ-based MTVs, although it has been reported
264 that the MTV of lung metastasis may be prognostic [18].

265 To our knowledge, the present study is the first to focus on measuring the MTV of DTC
266 patients in an organ-by-organ manner. This study is also an investigation of the largest number of
267 DTC patients regarding volume-based parameters of FDG-PET.

268 In clinical practice, we often encounter the following situation: two patients have almost
269 equivalent whole-body MTVs but have different prognoses as their metastatic organs differ. In
270 the relevant literature, metastasis to neck nodes has shown little relevance to prognosis in DTCs,
271 whereas metastatic brain or liver tumors lead to poor prognosis [11–13]. We thus propose that the
272 new indicator, the aMTV, has better prognostic power than the cMTV.

273 The results of our analyses demonstrated that some of the organ-based MTVs were
274 linearly correlated with the patients' OS while others were more closely correlated after
275 dichotomization. Several possible reasons for these results can be considered. Although it is
276 known that lung metastasis greatly affects the prognosis of thyroid cancer patients, the patients
277 with lung metastasis of DTC often have many small lesions in both lungs. In such cases, the
278 MTV_{lung} tends to be underestimated due to partial volume effects of PET, even though serum sTg

279 levels, which reflect the total tumor amount, are high. Notably, the present study involved old-
280 generation PET scanners, and the influence of the partial volume effect may thus have been
281 significant. Further investigations are needed to clarify whether the latest PET scanners with
282 improved resolution can improve the predictive value of MTV_{lung} .

283 In contrast, $MTV_{distant-node}$ and $MTV_{other-organs}$ as continuous variables were prognostic
284 factors, showing a linear correlation with OS. Unlike lung metastasis, those metastatic lesions
285 tend to be small in number but large in size. Such characteristics may be suitable for
286 measurement with PET.

287 We observed that cervical lymph node metastasis was poorly correlated with the DTC
288 patients' OS as a continuous variable. This is consistent with past reports that cervical lymph
289 node metastasis was not closely related to the prognosis of DTC [11]. However, we observed that
290 a strong correlation with the OS was obtained when the MTV_{neck} cut-off value was set to 2.9 mL
291 (equivalent to 1.8 cm in diameter), which is a relatively large volume for neck nodes, indicating
292 that even cervical nodes can affect the prognosis when the lesion is large.

293 There is no gold standard for MTV measurements in DTC. In general, for various tumors,
294 the tumor boundary is often determined using a relative value of 40% of the SUVmax or a fixed
295 value such as $SUV \geq 3.0$ as a threshold value. Since we targeted the whole body this time, it was
296 not practical to use a relative value of the SUVmax for many of the lesions in some cases. We
297 thus chose a fixed SUVmax. In the fixed value method, we considered several cut-off candidates
298 (e.g., 2.5, 3.0, and 3.5). Here, when we use values that are smaller than 2.5, much of the
299 background would be included inside the VOI and a considerable amount of manual correction
300 work would be required, which not only takes time but also reduces reproducibility between
301 operators. In contrast, when values that are larger than 3.5 are used, since thyroid cancer is a

302 basically low-accumulation tumor, the low-accumulation lesions could not be picked up in many
303 cases. We therefore used $SUV \geq 3.0$ as the threshold value for the empiric evaluation.

304 Prognostic indicators are useful in determining subsequent treatment strategies. In this
305 study, the aMTV was demonstrated to be an excellent prognosis indicator. A large aMTV was
306 associated with poor prognosis. Patients whose aMTV is large may therefore need careful
307 follow-up plus the introduction of aggressive treatment such as surgery to remove as much tumor
308 tissue as possible, external beam radiation therapy, and/or the use of molecular-targeted drugs
309 including TKIs. It may take time and effort to measure the organ-based MTVs at this point in
310 time, but artificial intelligence techniques will eventually make it possible to measure them
311 automatically and quickly.

312 There are several limitations of this study. It was a retrospective analysis enrolling patients
313 treated at a single institution, which inevitably biased the data selection. The prognosis of the
314 patients with thyroid cancer is generally good, but a long-term follow-up observation is required.
315 A prospective study of patients treated at several institutions is thus difficult to carry out,
316 although such a study is important. In addition, we did not investigate our patients' subsequent
317 treatments (further I-131 therapy, external irradiation, surgical dissection, etc.). The imaging
318 devices used for PET also differed among the patients. Although complicated, there is a method
319 of volume measurement that is able to harmonize images with different spatial resolutions; this
320 may be a future research subject. Moreover, although we preliminarily determined the weights of
321 organ-based MTVs, the weights ideally should be determined in as large a population as
322 possible. Finally, there were no confirmations by pathological examinations that metastasis was
323 present.

324

325 **Conclusion**

326 In patients with DTC with FDG-avid metastasis before I-131 therapy, all organ-based MTVs
327 were significant predictors of patient prognoses. The adjusted whole-body MTV may have the
328 potential to improve the performance of conventional MTV. Measuring the MTV by organ is
329 clinically meaningful.

330

331

332 **Acknowledgments**

333 We thank all staff in the nuclear medicine department of our hospital for their support with the
334 cyclotron operation, radiosynthesis, and image acquisition.

335

336 **Funding**

337 This work was supported by a grant from the JSPS KAKENHI, no. JP20K08015.

338

339 **Conflict of interest**

340 The authors declare that they do not have anything to disclose regarding funding or conflicts of
341 interest with respect to this manuscript.

342

343

344 **Figure Legends**

345

346 **Fig. 1.** We retrospectively enrolled 280 patients with DTC who underwent FDG-PET before their
347 initial I-131 therapy after undergoing a total thyroidectomy, and those who had any FDG-avid
348 metastases.

349

350 **Fig. 2.** A female patient in her 70s with multiple metastases of thyroid follicular cancer. The
351 metastatic lesions are displayed with different colors for each organ for the measurement of
352 organ-based MTVs.

353

354 **Fig.3.** Kaplan-Meier survival curves for the patients in the test group in relation to the aMTV **(a)**
355 and the cMTV **(b)**. Risk stratification was better achieved using the aMTV than the cMTV, up to
356 the sixth year (72 months) after PET scanning.

357

358 **Fig. 4.** The training dataset was analyzed with the time-dependent receiver operating
359 characteristic (ROC) curves in predicting (a) 1-year, (b) 3-year, and (c) 5-year survival using the
360 aMTV vs. the cMTV. The AUC was larger for the aMTV than for the cMTV in all of the
361 analyses.

362

363 **Fig. 5.** The validation dataset was analyzed with the time-dependent ROC curves in predicting
364 (a) 1-year, (b) 3-year, and (c) 5-year survival using the aMTV vs. the cMTV. The AUC was
365 larger for the aMTV than for the cMTV in all of the analyses.

366

367 **References**

- 368 1. Durante C, Haddy N, Baudin E et al. Long-term outcome of 444 patients with distant
369 metastases from papillary and follicular thyroid carcinoma: Benefits and limits of
370 radioiodine therapy. *J Clin Endocrinol Metab.* 2006;91:2892-2899.
- 371 2. Yang L, Shen W, Sakamoto N. Population-based study evaluating and predicting the
372 probability of death resulting from thyroid cancer and other causes among patients with
373 thyroid cancer. *J Clin Oncol.* 2013;31:468-474.
- 374 3. Yoshio K, Sato S, Okumura Y et al. The local efficacy of I-131 for F-18 FDG PET positive
375 lesions in patients with recurrent or metastatic thyroid carcinomas. *Clin Nucl Med.*
376 2011;36:113-117.
- 377 4. Gaertner FC, Okamoto S, Shiga T et al. FDG PET performed at thyroid remnant ablation has
378 a higher predictive value for long-term survival of high-risk patients with well-differentiated
379 thyroid cancer than radioiodine uptake. *Clin Nucl Med.* 2015;40:378-383.
- 380 5. Mantziari S, Pomoni A, Prior JO et al. 18 F- FDG PET/CT-derived parameters predict
381 clinical stage and prognosis of esophageal cancer. *BMC Med Imaging.* 2020 Jan 22;20(1):7.
- 382 6. Lovinfosse P, Polus M, Van Daele D, Martinive P et al. FDG PET/CT radiomics for
383 predicting the outcome of locally advanced rectal cancer. *Eur J Nucl Med Mol Imaging.*
384 2018 Mar;45(3):365-375.
- 385 7. Li Y, Wu X, Huang Y et al. 18 F-FDG PET/CT in lung adenosquamous carcinoma and its
386 correlation with clinicopathological features and prognosis. *Ann Nucl Med.* 2020
387 May;34(5):314-321.
- 388 8. Wang W, Larson SM, Fazzari M et al. Prognostic value of [18F]fluorodeoxyglucose positron
389 emission tomographic scanning in patients with thyroid cancer. *J Clin Endocrinol Metab.*

- 390 2000;85:1107-1113.
- 391 9. Kim BH, Kim S-J, Kim U et al. Diagnostic value of metabolic tumor volume assessed by
392 18F-FDG PET/CT added to SUVmax for characterization of thyroid 18F-FDG
393 incidentaloma. Nucl Med Commun. 2013;34:868-876.
- 394 10. Tam S, Boonsripitayanon M, Amit M et al. Survival in differentiated thyroid cancer:
395 Comparing the AJCC Cancer Staging Seventh and Eighth Editions. Thyroid. 2018;28):1301-
396 1310.
- 397 11. Brient C, Mucci S, Taïeb D et al. Differentiated thyroid cancer with liver metastases:
398 Lessons learned from managing a series of 14 patients. Int Surg. 2015;100:490-496.
- 399 12. de Figueiredo BH, Godbert Y, Soubeyran I et al. Brain metastases from thyroid carcinoma: A
400 retrospective study of 21 patients. Thyroid. 2014;24:270-276.
- 401 13. Collins GS, Reitsma JB, Altman DG et al., members of the TRIPOD group. Transparent
402 Reporting of a Multivariable Prediction Model for Individual Prognosis or Diagnosis
403 (TRIPOD): The TRIPOD Statement. Eur Urol. 2015;67:1142-1151.
- 404 14. Hirata K, Kobayashi K, Wong K-P et al. A semi-automated technique determining the liver
405 standardized uptake value reference for tumor delineation in FDG PET-CT. PLOS ONE.
406 2014;9:e105682.
- 407 15. Robbins RJ, Wan Q, Grewal RK et al. Real-time prognosis for metastatic thyroid carcinoma
408 based on 2-[18F]fluoro-2-deoxy-D-glucose-positron emission tomography scanning. J Clin
409 Endocrinol Metab. 2006;91:498-505.
- 410 16. Masson-Deshayes S, Schwartz C, Dalban C et al. Prognostic value of (18)F-FDG PET/CT
411 metabolic parameters in metastatic differentiated thyroid cancers. Clin Nucl Med.
412 2015;40:469-475.

- 413 17. Manohar PM, Beesley LJ, Bellile EL et al. Prognostic value of FDG-PET/CT metabolic
414 parameters in metastatic radioiodine-refractory differentiated thyroid cancer. *Clin Nucl Med.*
415 2018;43:641-647.
- 416 18. Maruoka Y, Baba S, Isoda T, Kitamura Y, Abe K, Sasaki M, Honda H. Association between
417 volumetric analysis of lung metastases on F-18-fluoro-2-deoxy-D-glucose positron emission
418 tomography/computed tomography and short-term progression after I-131 therapy for
419 differentiated thyroid carcinoma. *Indian J Nucl Med.* 2017;32(3):167-172.
- 420

Table 1. Characteristics of the 280 patients included in the study.

	Training	Test	p -value
Number of patients	190	90	
Gender			
male	66	27	0.4282
female	124	63	
Age			
range	13-84	14-80	0.573
(median, IQR)	(61.1, 56-70)	(60.0, 51.8-69)	
Pathology			
papillary	149 (78.4%)	80 (88.9%)	0.1661
follicular	23 (12.1%)	4 (4.4%)	
poor	15 (7.9%)	5 (5.6%)	
papillary + follicular	3 (1.6%)	1 (1.1%)	
Metastatic site			
neck lymph node	149 (78.4%)	72 (80.0%)	0.7632
distant lymph node	44 (23.2%)	25 (27.8%)	0.404
lung	95 (50.0%)	46 (51.1%)	0.8627
bone	30 (15.8%)	10 (11.1%)	0.2978
others	7 (3.7%)	3 (3.3%)	0.8831
Follow up period			
range	1.15-154.8	2.66-153.1	0.4042
(median, IQR)	(53.9, 25.2-92.6)	(56.6, 30.5-95.9)	
Outcome			
dead	51 (26.8%)	20(22.2%)	0.4084
alive	154 (73.2%)	74(77.8%)	
PET scanner			
EXACT47	95 (50.0%)	43 (47.8%)	0.8756
Biograph	85 (44.7%)	43 (47.8%)	
HR+	10 (5.3%)	4 (4.4%)	

Table 2. Univariate analysis

	Continuous value			Dichotomized value			
	p-value	Hazard ratio	95%CI	Cut-off	p-value	Hazard ratio	95%CI
MTV _{neck-node}	0.0763	1.016	[-0.0021, 0.028]	2.9	0.0258	2.004	[0.52, 1.84]
MTV _{distant-node}	0.0997	1.015	[-0.0038, 0.027]	0.3	0.0003	3.345	[0.58, 1.78]
MTV _{lung}	0.3059	1.002	[-0.0036, 0.0043]	1.5	0.0082	2.390	[0.23, 1.45]
MTV _{bone}	0.0060	1.014	[0.0048, 0.021]	15.5	0.0062	3.430	[0.39, 1.96]
MTV _{other-organs}	0.0011	1.012	[0.0057, 0.017]	0.1	0.0002	10.771	[1.28, 3.27]

Table 3. Multivariate analysis

	p-value	Regression coefficient	Hazard ratio	95% CI
d(MTV _{neck node})	0.308	0.69	2.096	[-0.681, 2.161]
MTV _{distant node}	0.018	0.02	1.039	[0.007, 0.070]
d(MTV _{lung})	0.002	1.05	7.084	[0.694, 3.222]
d(MTV _{bone})	0.065	1.58	7.560	[-0.128, 4.174]
MTV _{other-organs}	0.669	0.01	0.999	[-0.008, 0.005]

Fig. 1

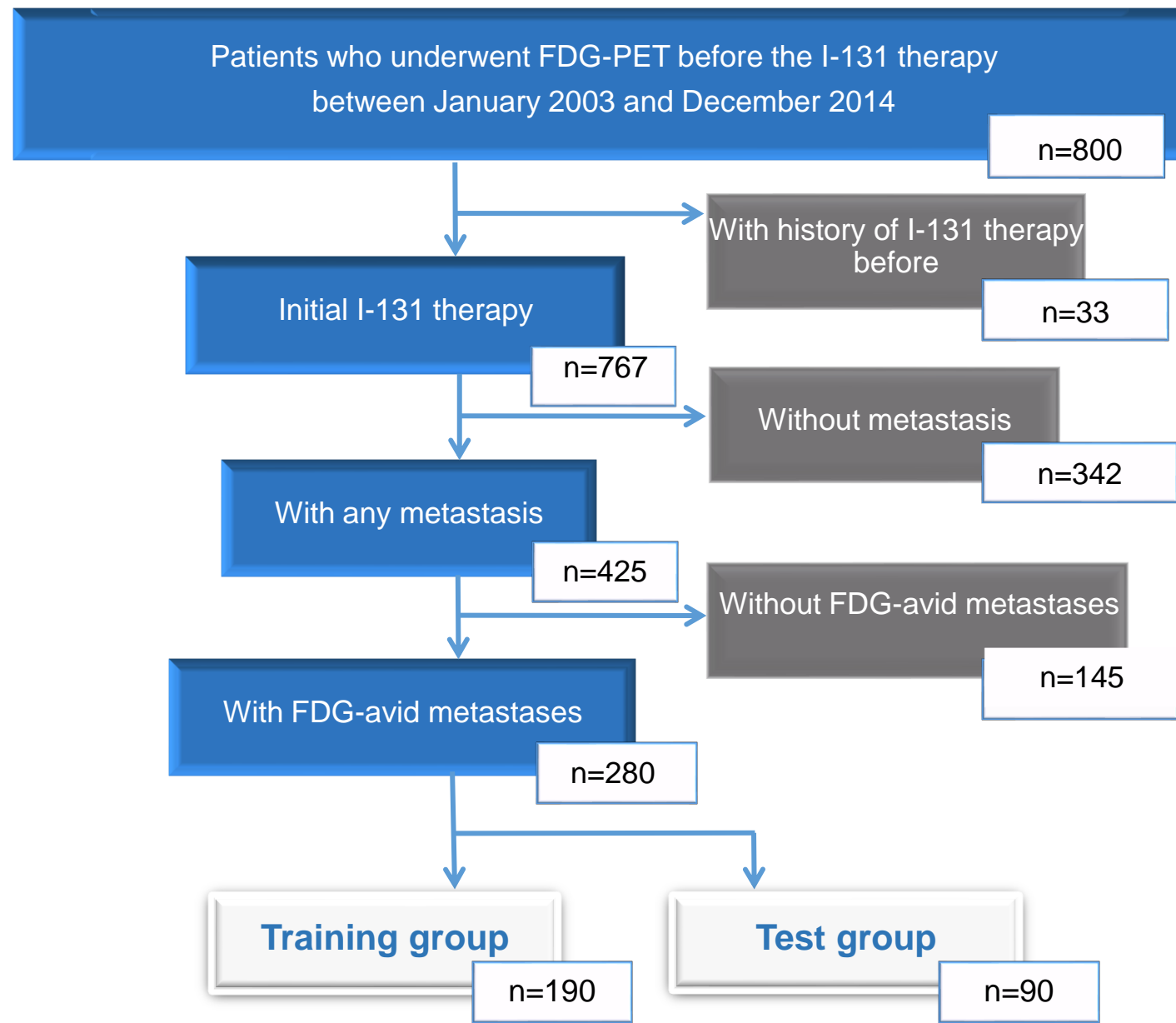
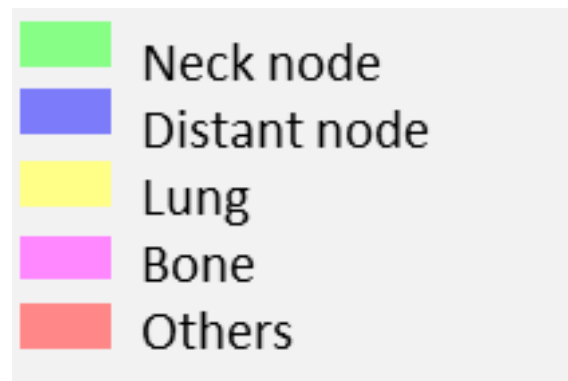
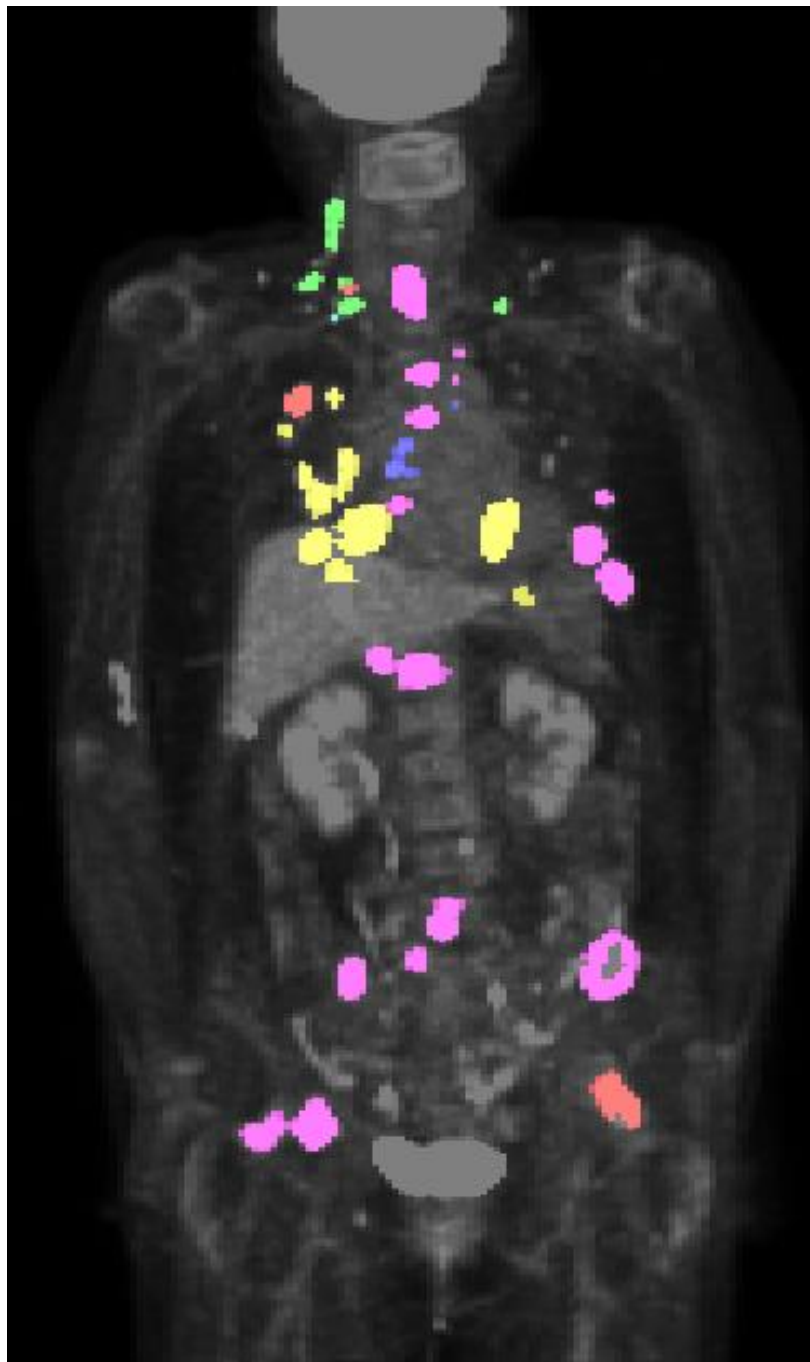


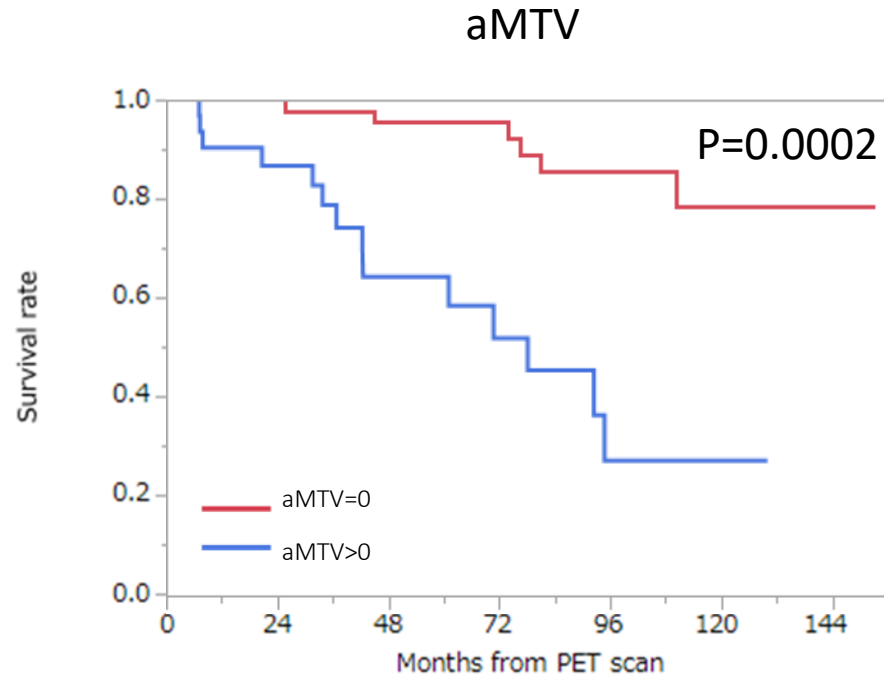
Fig. 2



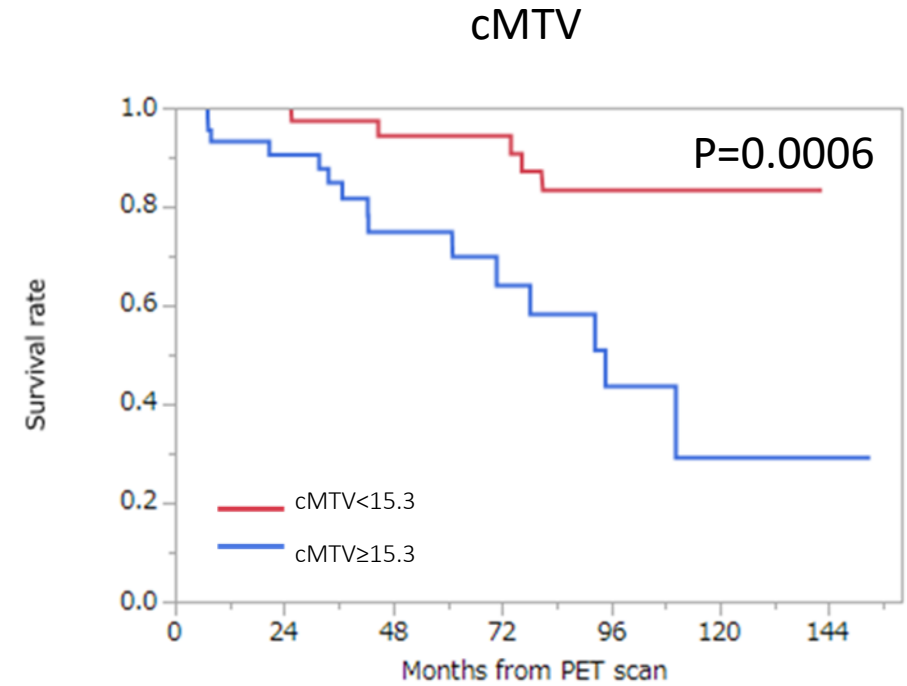
Region	MTV (mL)
Neck node	7.331
Distant node	2.992
Lung	52.283
Bone	134.629
Others	17.451
All	214.686

Fig. 3

a



b



Total o. of patients	90	74	53	39	24	13	2
aMTV=0	58	49	40	30	21	11	2
aMTV>0	32	25	13	9	3	2	0

Total o. of patients	90	74	53	39	24	13	2
cMTV<15.3	45	39	31	27	18	10	1
cMTV≥15.3	35	35	22	12	6	3	1

Fig. 4

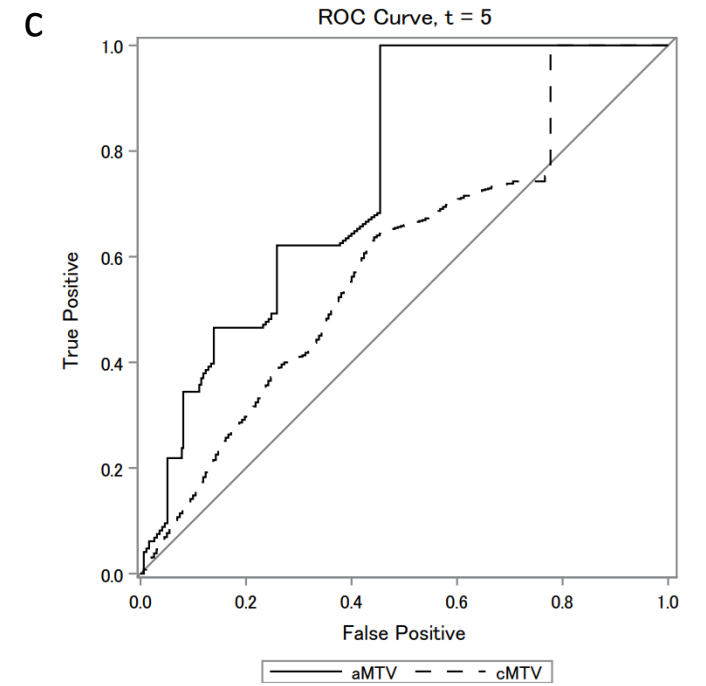
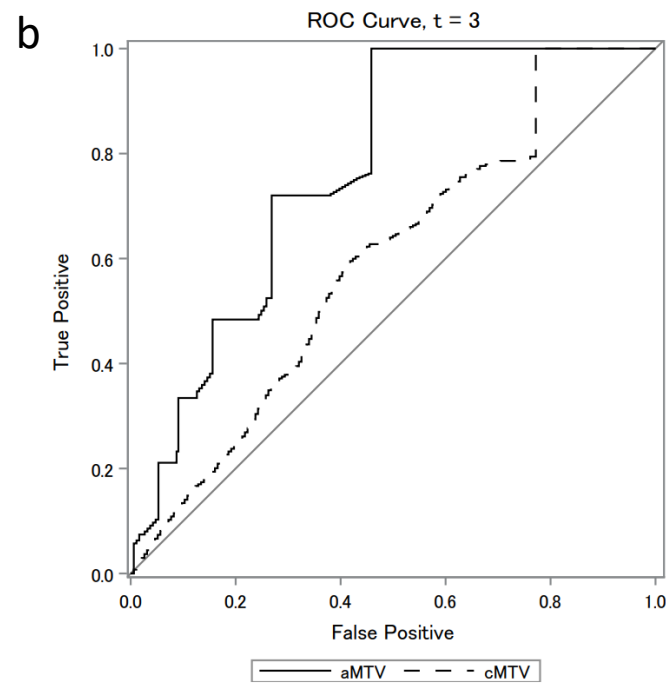
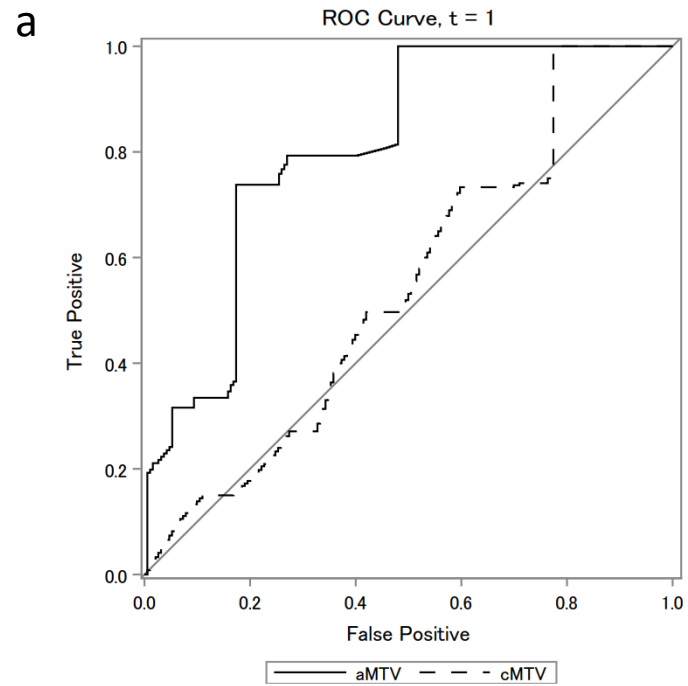


Fig. 5

